EXPERIMENTAL INVESTIGATION ON THE EFFECT OF AIR IN PUMPING NON-SETTLING FLUIDS

N. Zanini[*] - *A. Suman*[*] - *M. Pinelli*[*] - *J. F. Gülich*[+]

* University of Ferrara - Department of Engineering, Via Saragat 1, 44122, Ferrara, Italy
+ Independent Consultant, Villeneuve, Switzerland

ABSTRACT

Non-Newtonian fluids are involved in many industrial processes, e.g. in food and Oil&Gas applications. Since their viscosity varies with the imposed stress and rheology, pumping this type of fluids can lead to a considerable variation in the pump head, and overall efficiency is difficult-to-be-predicted. Since most manufacturers test their pumps only with water, selecting the appropriate pump to handle non-settling slurries may be challenging due to the non-linear effects, related to the fluid rheology and the critical interaction with the air bubbles. In this work, an experimental investigation was carried out on an on-purpose test bench, testing two mixtures of water and kaolin on a small centrifugal pump. The fluids were tested at two degrees of air bubbles content: an initial aerated condition and after a deaeration process. A critical analysis was conducted to relate the experimental pump performance variation with the air bubbles content.

KEYWORDS

Centrifugal Pumps, Non-Newtonian Fluids, Oil&Gas, Slurry Transport, Non-Settling Fluids, Air Bubbles

NOMENCLATURE

C mechanical torque $[Nm]$
C_n mechanical torque without fluid $[Nm]$
H pump head $[m]$
k consistency index $[Pa\ s^n]$
n flow index [-]
P_i inner power [W]
p_d discharge static pressure $[Pa]$
p_s suction static pressure $[Pa]$
Q volumetric flow rate $[m^3\ s^{-1}]$
$q*$ flow rate referred to flow rate at best efficiency point [-]
v_d discharge nozzle velocity $[m\ s^{-1}]$
v_s suction nozzle velocity $[m\ s^{-1}]$
z_d pump discharge height $[m]$
z_s pump suction height $[m]$
$\dot{\gamma}$ shear rate $[s^{-1}]$
η inner efficiency [%]
ρ mixture density $[kg\ m^{-3}]$
τ shear stress $[Pa]$
τ_0 yield stress $[Pa]$
ω rotational speed $[rad\ s^{-1}]$

INTRODUCTION

Centrifugal pumps are widely employed to handle fluids in many industrial processes due to their high reliability, robustness, and large flow rates at an affordable price. The choice of the appropriate pump for a pipeline or a plant is carried out employing the performances given by manufacturers, which are usually obtained with water. Besides that, high efficiencies must be guaranteed to prevent excessive operating costs. Difficulties in choice emerge when highly viscous or non-Newtonian fluids have to be managed, such as in mining and food processes (Wilson et al. (2006)), and no information about the performance with this kind of fluids is provided.

While several methods can be found in the literature to derate the pump performance with water to that with high viscous fluids (ANSI-HI 9.6. 7-2010 (2010), Paternost et al. (2015), Ofuchi et al. (2020)), no general method can be employed for non-Newtonian fluids and no detailed information is provided in terms of pump-fluid behavior interaction. In particular, previous test with non-settling slurries (Walker and Goulas (1984), Kabamba (2006), Occari et al. (2019b)) reported instabilities at low flow rates difficult-to-be-modeled. However, some modeling attempts have been made (Walker and Goulas (1984), Pullum et al. (2007), Sery et al. (2006)) and, accepting a wide range of uncertainty, it is possible to obtain a derated pump curve. The performance impairment caused by non-settling slurries was also analyzed by Kalombo et al. (2014), Sellgren et al. (2011), and Occari et al. (2019a) generating a set of literature data based on different pumps and fluids. Moreover, for this kind of fluid, the tendency to absorb air in the mixture is particularly strong, and consequently, fluid rheology is not the only critical aspect.

Most industrial processes occur in turbulent flow regimes, entailing vortices and promoting the formation of bubbles (Wilson et al. (2006)). For low-viscosity fluids, bubbles can easily spill from the flow while for higher viscosity values the viscous forces overcome the inertial ones leading to the air bubbles trapping. The complex nature and rheology of non-settling slurries do not allow to predict their viscosity during their handling in industry and, consequently, their affinity in trapping air bubbles can not be well predicted. In light of this, the study of the generation of the bubbles and dynamics in non-Newtonian fluids is of primary importance to guarantee the reliability of these processes, as reported by Li (1999), Chhabra (2006), and Funfschilling and Li (2001). Furlan et al. (2013) reduced the air content of three paste slurries purging air in an uncontrolled way before conducting tests with a centrifugal pump. The authors reported that no instabilities were detected for the deaerated slurries suggesting that air bubbles are responsible for the drops in performance typical of non-settling fluids. From these considerations, further experimental investigations are necessary to establish a relation between the pump performance and the air bubbles content in the fluid. In this work, an experimental campaign with two non-settling mixtures in an on-purpose test bench was carried out for a small commercial centrifugal pump, monitoring the air bubbles contained in the fluids. The capability of the air bubbles control allows the establishment of a relation between non-Newtonian fluid behavior, air bubbles, and pump performance. Several tests with different pump rotational speeds have been carried out providing a specific pump characterization useful to highlight general guidelines in the air bubble and non-settling fluid interaction.

EXPERIMENTAL APPARATUS

Tests were carried out on an on-purpose test bench to evaluate the influence of the air bubbles in non-Newtonian fluids on the pump performance. In particular, the closed test loop with

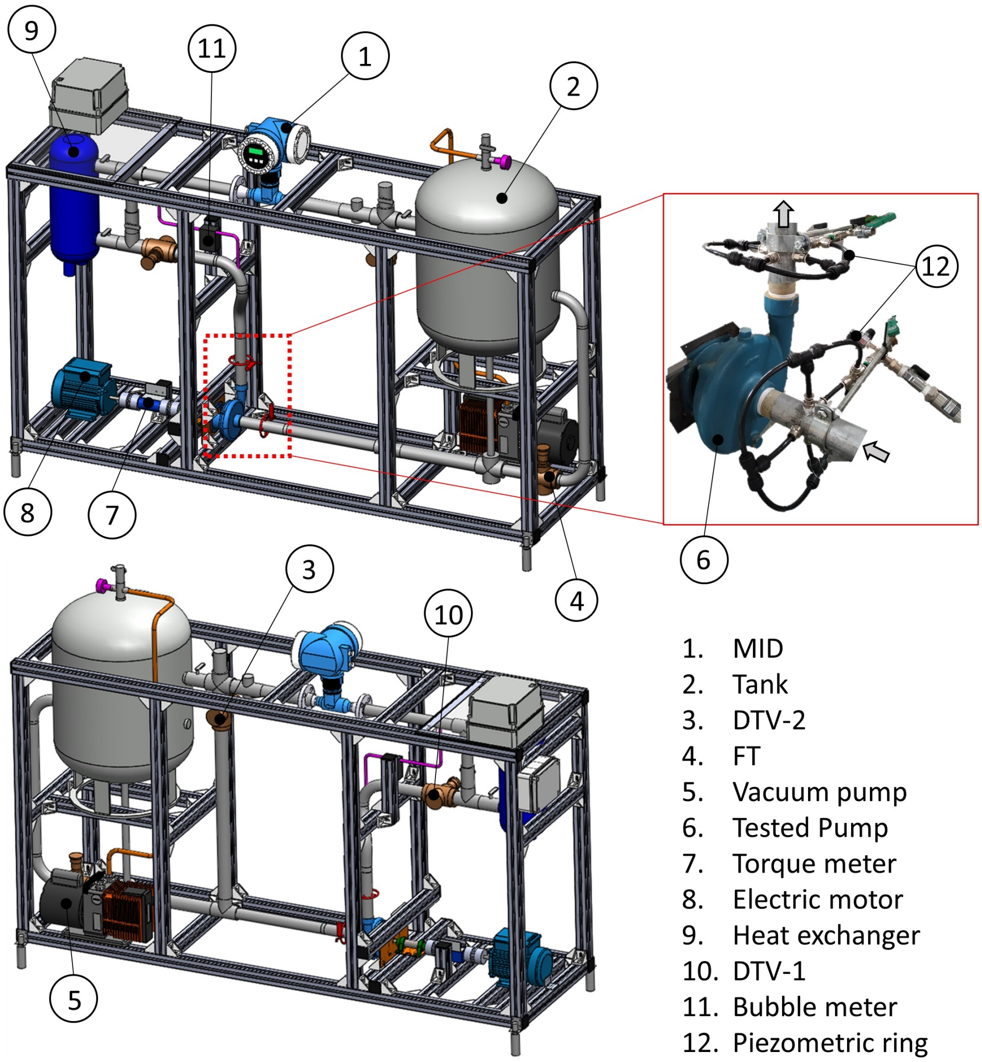

Figure 1: **Test bench model**

pressurizer described by Gülich (2020) was taken as a reference. A schematic representation of the test rig is reported in Fig.1.

The main loop comprises galvanized steel pipes with an outer diameter of 48.3 mm, and 3.3 mm thick. A 100 liters tank guarantees the reservoir during the test. The constant fluid temperature during operations is guaranteed by means of a tube bundle heat exchanger (HE). The tested pump is actuated by a 0.55 kW inverter-driven electric motor (EM), and a BURSTER 86-2112R-5020 torque meter (TM) is interposed between the motor shaft and the pump shaft, whose uncertainty is $\pm$ 0.04 Nm. The rotational speed is measured with a magnetic pickup that overlooks the electric motor fan. The volumetric flow rate is measured employing an electromagnetic flowmeter Endress+Hauser Proline Promag 55S (MID) which has an uncertainty of $\pm$ 0.2 %R. According to the ISO 9906:2012 (2012) standard, the measuring sections are located two diameters away from the suction and the discharge flanges to compute the pump head. Each section is equipped with an absolute pressure transducer. A Measurement Specialties Pressure sensor U5131 (range of 0-2 bar) for the suction and a Measurement Specialties Pressure sensor US381 (range 0-6 bar) for the discharge section. An uncertainty calculation based on the procedure reported in the standard ISO/IEC Guide 98-3:2008 (ISO 98-3:2008 (2008)) and EA-4/02M (JCGM (2008)) is performed in order to estimate the uncertainty of the pressure measurement. The two pressure transducers and the correspondent measurement chain have been calibrated at the same time employing the pressure calibrator MicroCal PM200+, representing the in-house laboratory secondary standard which, in turn, is calibrated towards a primary laboratory standard certified in agreement with the Italian Accreditation Body (Accredia). The type B uncertainty is obtained by considering the uncertainty of the primary laboratory standard as the reference uncertainty U_{PLS} and the residual uncertainty value of the pressure measurement chain E_R. The first (U_{PLS}) is supposed Gaussian distributed and consequently it is divided by 2 for calculating the standard deviation equivalents, while the latter (E_R) is estimated considering the difference between the reference value (also called the true value) and the average value of the signal provided by the measurement chain reordered for 2 s under a constant pressure input (generated and controlled by the MicroCal PM200+). This term is considered to have a rectangular probability distribution and for this reason, it is divided by $3^{1/2}$. Finally, the evaluation of the type A uncertainty is carried out by estimating the standard deviation (considered as a Gaussian distribution, and for this reason, it is divided by 2 for calculating the standard deviation) of the data set U_σ. The final assessment of the pressure measurements uncertainty is performed in Eq.1.

$$\delta p = \sqrt{\left(\frac{U_{PLS}}{2}\right)^2 + \left(\frac{E_R}{\sqrt{3}}\right)^2 + \left(\frac{U_\sigma}{2}\right)^2} \tag{1}$$

A K-type thermocouple is also provided for the suction and discharge sections. The measured values of pressure and temperature are the average of four equally distributed taps joint by a piezometric ring, as reported in Fig.1. The pressure transducers are arranged horizontally to prevent from the air and solid particles trapping in the instrument lines. Another K-type thermocouple is placed in the tank to monitor the temperature of the reservoir fluid. A pneumatic valve system at the top of the tank allows to supply or suck the air bubbles from the liquid stored in the loop. The ambient pressure can be established by opening the vent valve, while, by means of a screw compressor and a vacuum pump, it is possible to increase or reduce the tank pressure. In addition, a SONOCHECK-ABD06 bubble meter (BM) is installed next to the pump discharge section to evaluate the air bubbles content inside the tested fluid. This non-invasive sensor is commonly employed for medical applications, e.g., to monitor the presence of bubbles during blood transfusions or dialysis by means of the ultrasound principle (Leung et al. (2021)), or biotechnology processes (Roth et al. (2016)). The ultrasound wave emitted by the device crosses the measuring section (pipe) and depending on the transit time to reach the receptacle, an analog output is produced. Its signal is processed by internal algorithms, and it returns a signal proportional to the size of the bubbles detected. As declared by the manufacturer, the device is able to detect bubbles with a characteristic length up to 1/3 of the internal diameter of the pipe considered. A branch from the main loop with a transparent plastic pipeline with an internal diameter of 4 mm is arranged to meet the installation requirements of the instrument. All signals from the measuring sensors and the control signals for the motorized valves are managed by a NI DAQ hardware system through software specifically developed in the LabVIEW environment.

Two different loop operative configurations can be alternately employed using three actuated valves (DTV-1, DTV-2, FV). In the "open-loop" scheme (Fig.2a), the DTV-2 is completely

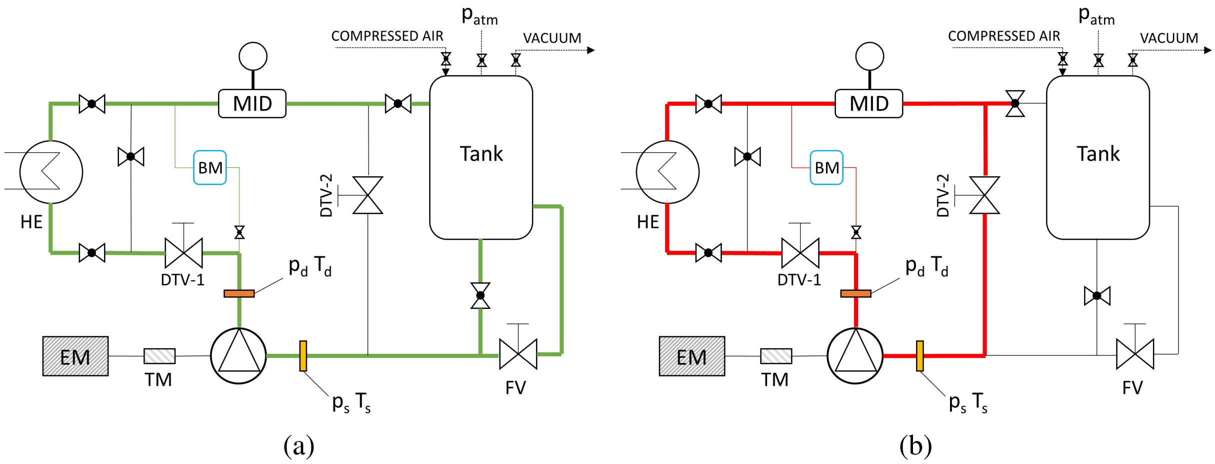

Figure 2: **Loop operative configurations - (a) Open-loop; (b) Closed-loop**

N [rpm]	2900
Q_{BEP} [l/s]	1.55
H_{BEP} [m]	18.5
n_q [rpm $m^{0.75}/s^{0.5}$]	12.8
D_{imp} [mm]	119.5
Z	7
Impeller axial clearance [mm]	1
Ra impeller [µm]	3.15

Figure 3: **Tested pump dimensions and performance with water**

closed, and the fluid flows through the tank before reaching the pump suction. In the "closed-loop" scheme (Fig.2b), the tank is insulated by closing the FV and opening the DTV-2, and an additional vent valve is placed next to the MID. DTV-1 valve is employed in both schemes to change the flow rate inside the loop. The employment of the closed-loop is suggested to handle less volume fluid.

EXPERIMENTAL CAMPAIGN

Pump Tested

In this experimental campaign, the same open-impeller *Pump B* tested by Occari et al. (2019b) is considered. Its characteristics and performance with water are summarized in Fig.3. Hydraulic connections and flexible pipes are added to join the main loop and the 1" diameter pump suction and discharge sections.

Fluids Characterization

Two mixtures of water and kaolin powder of 35% and 40% of solid content are tested in the present work. The density of the fluids was calculated by weighing a measuring cylinder filled with the fluid with a capacity of 100 ml and uncertainty of ± 0.5 ml. The measurements have been performed with the Kern ABT 100-5NM analytical scale (Kern, Balingen, Germany). The

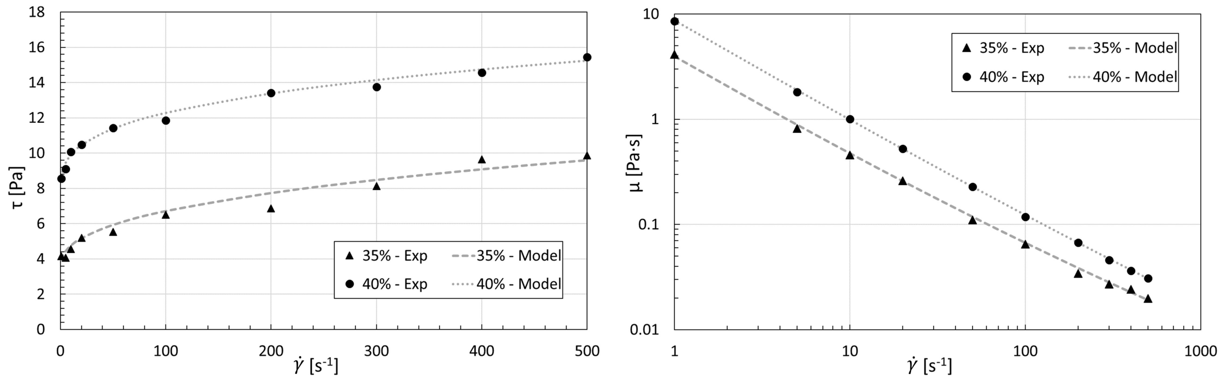

Figure 4: **Kaolin mixtures rheology**

Kaolin Mixture [wt%]	$\rho\ [kg\ m^{-3}]$	$\tau_0\ [Pa]$	$k\ [Pa\ s^n]$	$n\ [-]$
35	1207	3.4	0.55	0.39
40	1238	7.5	1.2	0.30

Table 1: **Water and kaolin mixtures densities and rheological model coefficients**

procedure was repeated three times for each mixture and the resulting average density values are reported in Tab.1. Rheological data were obtained with the rotational rheometer Rheometric Scientific ARES-LS equipped with 25 mm titanium parallel disks with a gap between the plates set to 1 mm. The rheological characterization is carried out for the range of shear rate $[1 - 500\ s^{-1}]$ five times for each mixture, and the resulting average shear stress and dynamic viscosity are reported in Fig.4. The uncertainty for the shear stress and the dynamic viscosity is estimated to be the $\pm$ 3% and the $\pm$ 5% of the measured values respectively.

The non-Newtonian fluid behavior emerges clearly from the experimental data. In detail, both the mixtures belong to the shear-thinning fluid category, and the Herschel-Bulkley model is chosen as the most appropriate to outline their rheology. Therefore, the relation between shear rate and shear stress acting on the fluid assumes the following form:

$$\tau = \tau_0 + k\dot{\gamma}^n \qquad (2)$$

where τ_0 is the yield stress, k is the consistency index, and n is the flow index. The coefficients of the rheological model for each mixture are obtained from the best fitting of the experimental data and are summarized in Tab. 1.

Test Method

The present experimental campaign aims to investigate the influence of the air trapped inside two different water/kaolin mixtures on the performance of the centrifugal pump described above. All the tests were performed passing through the reservoir, i.e., using the *open-loop* layout (Fig.2a), to employ the vacuum pump and reduce the air bubbles content of the tested fluids. The tests are conducted at three constant rotational speeds (2900, 2500, and 2000 rpm), changing the flow rate utilizing DTV-1. Initially, performance tests with water have been carried out as a reference condition. Then, the performance tests with kaolin mixtures are performed at two different grades of air content: an initial *aerated* condition, and a *deaerated* one.

The test procedure for a water/kaolin mixture is summarized in the following steps:

1. **Preparing the mixture**. The kaolin powder and water are weighed and then poured together in jerry cans producing eighty liters of mixtures. A small amount of fluid is spilled to measure its density and doing the rheological characterization. The loop is then filled with the prepared fluid.

2. **Aerated test**. The mixture is circulated through the loop for thirty minutes setting the pump rotational velocity at 2900 rpm to increase the air fraction (bubbles) in the liquid. During this phase, the degree of aeration is evaluated using the bubble meter (BM) and through visual inspection from the top of the tank. Preliminary tests reported that the water/kaolin mixtures are inclined to hold bubbles. Besides, thirty minutes of fluid processing in these conditions are adequate to guarantee a high level of bubbles generation in the loop. Finally, the pump performance are evaluated at constant speed changing the flow rate by means of the DTV-1.

3. **Deaerated test**. The vacuum pump is activated to suck the air bubbles from the tested fluid. To uniform the effect of the deaeration process, the tested pump remains activated during this phase with a speed set to 1500 rpm, which corresponds to an approximated fluid velocity of 0.8 m/s. The signal of the bubble meter is taken as a reference to evaluate the effectiveness of the deaeration process. Preliminary tests reported that the bubble meter signal decreases while the vacuum pump is working, and almost five minutes are sufficient to obtain a regular, not decreasing signal. In Fig.5a the bubble meter signals produced by water and a 40%wt. water/kaolin mixture are compared for an acquisition time of 120 s. The signal reported in the axis ordinate, represents the bubble intensity within the fluid derived from the acoustic behavior of the fluid. It appears clear that the presence of suspended particles in the mixture increases the average signal and amplitude with respect to water. Besides, the deaerated 40%wt. kaolin/water mixture shows a reduced average signal and wave amplitude compared to the aerated one. This reflects the lower amount of air bubbles in the mixture after deaeration. In Fig.5b the deaerated 40%wt. and 35%wt. mixtures are compared, reporting slight differences in the acquired waves. Among these, the 40%wt. mean signal appears higher than the 35%wt. ones. Once the deaeration process is finished, before conducting the pump performance tests, the ambient pressure is established in the loop by opening the vent valve at the top of the tank. The obtained experimental results are then compared with the aerated ones.

RESULTS

Through the measurements, the pump head (H), the inner power (P_i) and the inner efficiency (η) are calculated as follows:

$$H = \frac{p_d - p_s}{\rho g} + \frac{v_d^2 - v_s^2}{2g} + (z_d - z_s) \tag{3}$$

$$P_i = (C - C_n)\omega \tag{4}$$

$$\eta = \frac{\rho Q g H}{P_i} \tag{5}$$

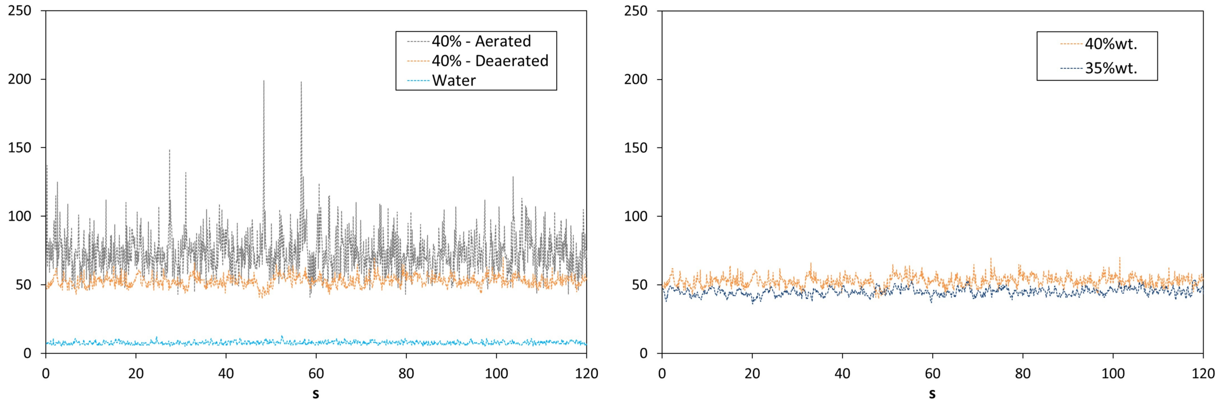

(a) (b)

Figure 5: **Bubble meter signal for a pump velocity of 2900 rpm - (a) 40%wt. before and after deaeration; (b) 40%wt. vs. 35%wt. deaerated mixtures**

where p_d and p_s are the static pressure at the pump discharge and suction, respectively, ρ is the fluid density, z_d and z_s are the heights of the measuring sections at the pump discharge and suction, Q is the volumetric flow rate, ω is the rotational speed, C is the mechanical torque, and C_n is the necessary torque to overcome the mechanical friction in the bearings and the shaft seal. C_n was measured before starting the test without fluid in the loop. Since the suction and the discharge nozzle have the same diameter, velocity heads cancel. The propagation of the uncertainty is realized by employing the procedure based on propagation rules (ISO 98-3:2008 (2008)), which allows calculating the expanded uncertainty u_c for a given variable y as follows:

$$u_c(y) = \sqrt{\sum_{i=1}^{N} \left(\frac{df}{dx_i}\right)^2 u^2(x_i)} \tag{6}$$

where x_i are the dependent variables of the f function, which define the variable y, and $u(x_i)$ is the uncertainty related to each dependent variable evaluated as done for the pressure measurements in Eq.1. As a result from the uncertainty evaluation, the magnitude of the extended uncertainty of the measurement chains (pressure, flow and torque meter) is reported by the marker width. The resulting performance at different rotational speed are plotted against the flow rate for the two water/kaolin mixtures and water in Fig. 6.

The pump head obtained with the kaolin/water mixtures at high flow rates overcomes the water one. This phenomenon called the *sudden-rising-head effect*, was previously investigated by several authors in literature (Li (2011), Aldi et al. (2017), Buratto et al. (2017)) and it can occur handling Newtonian fluids slightly more viscous than water. When it takes place, both the head and the inner efficiency obtained for the mixtures exceed the performance with water. The inner efficiency with the viscous fluids under the aerated condition at 2000 rpm and 2500 rpm report an increment up to 5% of the efficiency with water at high flow rates. This result is in line with the outcomes of Li (2011) and Aldi et al. (2017). As seen in other publications with non-settling slurries with air entrainment, the curves for aerated mixtures at 2900 rpm deviate from the water most at part load; they intersect the water curve at flow rates which increase with the kaolin concentration: with 35% at q* = 0.85 and with 40% at q* = 1.23. At flows higher than these intersections head and efficiency with the kaolin mixture measured were higher than

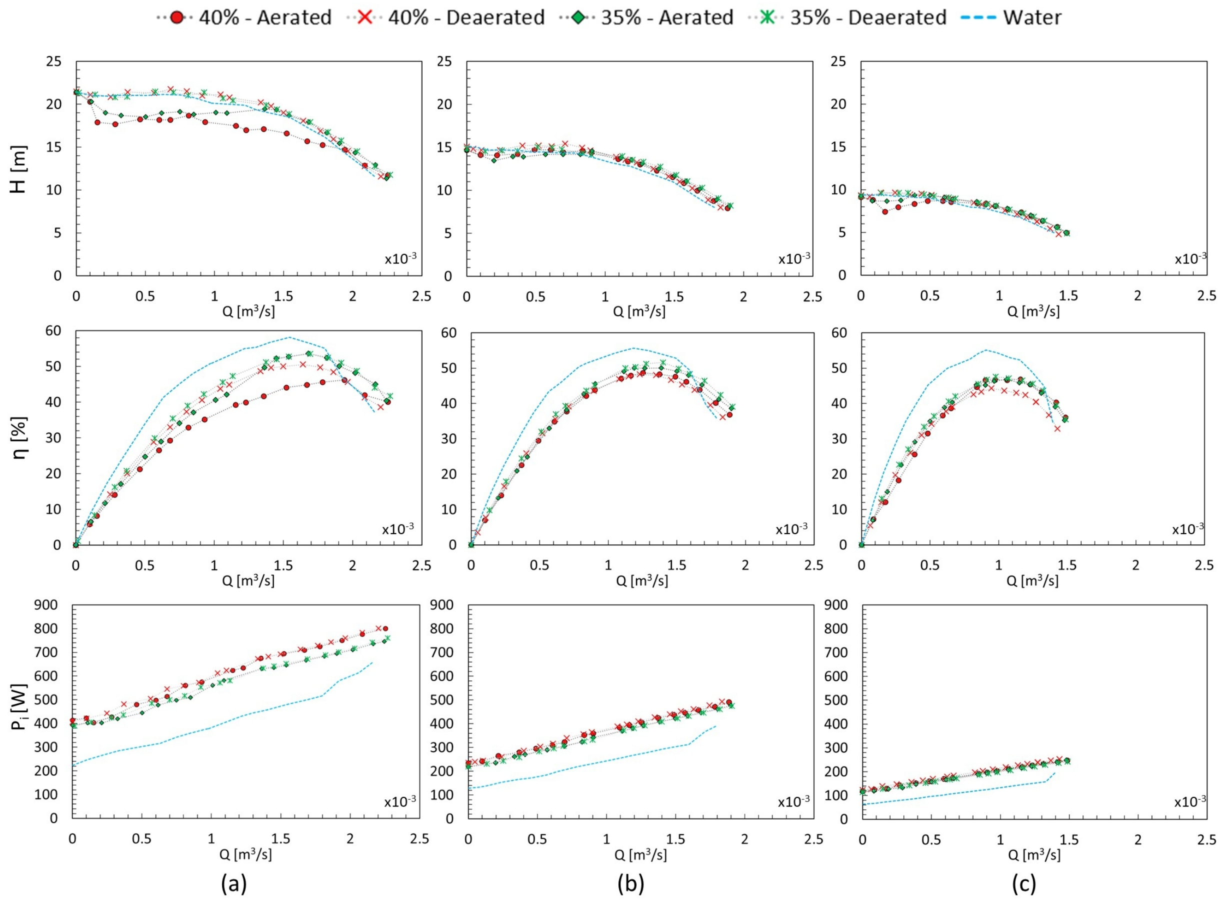

Figure 6: **Experimental pump performance - (a) 2900 rpm; (b) 2500 rpm; (c) 2000 rpm**

with water. This apparent improvement increased with q*. It was 8% in the head at q* = 1.37 with 35% but negligible with 40%.

It appears clear that the presence of air bubbles in the fluid strongly influences the pump performance. For both the mixtures, the aerated tests report a drop in the pump head and inner efficiency for low volumetric flow rates. Higher kaolin concentrations correspond to greater drops, and increasing the rotational speeds leads to an extension of the unstable curve area. On the other hand, the deaerated tests show no head instabilities at all the flow rates, resembling Newtonian behavior. Besides, the inner efficiency increases when the mixture is de-aerated. At constant rotational speed, for high flow rates, the deaerated head curves match the aerated ones, and the sudden-rising-head effect is still detected. Therefore, different air content in the same fluid corresponds to different behavior only at low flow rates when instabilities arise due to the presence of air bubbles. In light of this, higher kaolin concentrations promote greater bubble trapping, and consequently, more bubbles are detected during tests. Experimental data also reported that the discharge pressure trend follows the head one, so, the drops at low flow rates could be ascribed to the compressibility effects introduced by the air bubbles that change their characteristics (density and, thus, the occupied volume) over the pump. The compressibility effects due to the presence of air bubbles within the fluid generate a modification of the pressure value at the pump discharge section (Fig.7a), while the pressure at the suction seems not to be affected by the air content (Fig.7b). At the same, comparing the different rotational

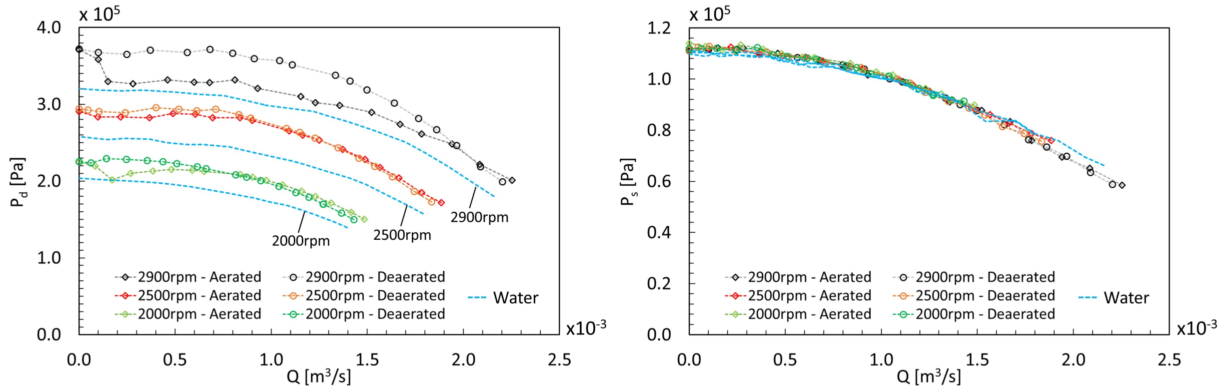

(a) (b)

Figure 7: **Water vs. Kaolin mixture 40%.wt - (a) Discharge pressure; (b) Suction pressure**

speeds (see Fig.7a), this phenomenon is not triggered in a non-trivial way by the pressure but it is a combination of pump operating point (i.e. rotational velocity and flow rate), and fluid characteristics (i.e. solid particles and air bubble contents). The effect of free gas in water is reported by Gülich (2010) for different gas volume fractions, where the same type of instability observed in the present study was detected. However, instability in water establishes at $q^* > 1$, contrary to the tests with kaolin mixtures. This could be ascribed to the lower sensitivity of the semi-open impellers to gas than the closed impellers.

CONCLUSIONS

In this work, an experimental campaign was carried out in an on-purpose test rig on a small centrifugal pump to investigate the influence of air bubbles in pumping non-Newtonian fluids. Two different kaolin/water mixtures were tested under aerated and deaerated conditions. A bubble meter was employed to evaluate the air bubble content in the mixtures before testing. As a result, increasing the kaolin concentration in the mixture, the pump performance curves become more unstable, reflecting an increasing presence of bubbles in the fluid. Drops in the pump head are experienced at low flow rates for the aerated test while the deaerated ones seem not to be affected by the residual air influence. The sudden-rising-head effect occurs for both the tested mixtures and it corroborates the viscous head and efficiency higher than the water ones. The observed rise in pump head with viscous fluids can be caused by reduced leakage around the blades of the semi-open impeller but further investigations are needed.

Future efforts will be devoted also to testing non-settling fluids with different rheology than the ones tested in this work, under deaerated conditions. Although the tested mixtures have non-Newtonian rheological characteristics, the performance obtained after the deaeration process is Newtonian-like, suggesting that the held air bubbles are responsible for the instabilities at partial load found in the literature. The reliability of the derating methods from literature, e.g. the Hydraulic Institute, should be tested with the deaerated mixtures. As consequence, the instabilities of the pump performance should be modeled only as a function of the air bubbles locking affinity of the tested fluid.

ACKNOWLEDGEMENTS

The authors want to thank Dr. Valentina Mazzanti, from the Department of Engineering of Ferrara for having conducted the rheology characterization of the kaolin/water mixtures; Mr. Andrea Gibelli, from Repcom s.r.l., for his valuable support in using the bubble meter.

REFERENCES

Aldi, N., Buratto, C., Casari, N., Dainese, D., Mazzanti, V., Mollica, F., Munari, E., Occari, M., Pinelli, M., Randi, S., Ruggero Spina, P., and Suman, A. (2017). Experimental and numerical analysis of a non-newtonian fluids processing pump. *Energy Procedia*, 126:762–769.

ANSI-HI 9.6. 7-2010, H. (2010). Effects of liquid viscosity on rotodynamic (centrifugal and vertical) pump performance. *Hydraulic Institute*.

Buratto, C., Occari, M., Aldi, N., Casari, N., Pinelli, M., Spina, P., and Suman, A. (2017). Centrifugal pumps performance estimation with non-newtonian fluids: Review and critical analysis. *12th European Conference on Turbomachinery Fluid Dynamics and Thermodynamics, ETC 2017*.

Chhabra, R. P. (2006). *Bubbles, drops, and particles in non-Newtonian fluids*. CRC press.

Funfschilling, D. and Li, H. Z. (2001). Flow of non-newtonian fluids around bubbles: Piv measurements and birefringence visualisation. *Chemical Engineering Science*, 56(3):1137–1141.

Furlan, J., Visintainer, R., and Sellgren, A. (2013). Pumping a 100–600 pa yield stress clay slurry with a centrifugal pump. In *Paste 2013: Proceedings of the 16th International Seminar on Paste and Thickened Tailings*, pages 531–543. Australian Centre for Geomechanics.

Gülich, J. F. (2010). Influence of the medium on performance. In *Centrifugal Pumps*, pages 741–808. Springer.

Gülich, J. F. (2020). Pump testing. In *Centrifugal Pumps*, pages 1205–1230. Springer.

ISO 98-3:2008 (2008). Uncertainty of measurement part 3: guide to the expression of uncertainty in measurement. Standard, International Organization for Standardization, Geneva, CH.

ISO 9906:2012 (2012). Rotodynamic pumps - Hydraulic performance acceptance tests - Grades 1, 2 and 3. Standard, The British Standards Institution.

JCGM (2008). Evaluation of measurement data Guide to the expression of uncertainty in measurement. Standard, International Organization for Standardization, Geneva, CH.

Kabamba, B. M. (2006). *Evaluation of centrifugal pump performance derating procedures for non-Newtonian slurries*. PhD thesis, Cape Peninsula University of Technology.

Kalombo, J., Haldenwang, R., Chhabra, R., and Fester, V. (2014). Centrifugal pump derating for non-newtonian slurries. *Journal of Fluids Engineering, Transactions of the ASME*, 136(3).

Leung, E., Meah, K., Moscola, J., Hake, D., Bosse, R., Sperbeck, C., Wickard, C., Owrutsky, J., Graf, K., Acierno, R., Wright, A., Mickenberg, J., and Smeltzer, H. (2021). Design of an automated bubble detection device for neuroangiography.

Li, H. Z. (1999). Bubbles in non-newtonian fluids: Formation, interactions and coalescence. *Chemical Engineering Science*, 54(13-14):2247–2254.

Li, W. (2011). Effect of exit blade angle, viscosity and roughness in centrifugal pumps investigated by cfd computation. *Task quarterly*, 15(1):21–41.

Occari, M., Mazzanti, V., Mollica, F., Munari, E., Pinelli, M., and Suman, A. (2019a). Numerical simulations of a centrifugal pump with a non-newtonian fluid: Influence on performances of different rheological modelling. *ASME-JSME-KSME 2019 8th Joint Fluids Engineering Conference, AJKFluids 2019*, 2.

Occari, M., Pinelli, M., Munari, E., Mollica, F., Mazzanti, V., and Suman, A. (2019b). Experimental tests with centrifugal pumps: Degradation of performance, instability and dynamic phenomena with non-newtonian suspensions of kaolin in water. volume 3B-2019.

Ofuchi, E., Cubas, J., Stel, H., Dunaiski, R., Vieira, T., and Morales, R. (2020). A new model to predict the head degradation of centrifugal pumps handling highly viscous flows. *Journal of Petroleum Science and Engineering*, 187.

Paternost, G., Bannwart, A., and Estevam, V. (2015). Experimental study of a centrifugal pump handling viscous fluid and two-phase flow. *SPE Production and Operations*, 30(2):146–155.

Pullum, L., Graham, L., and Rudman, M. (2007). Centrifugal pump performance calculation for homogeneous and complex heterogeneous suspensions. *Journal of the Southern African Institute of Mining and Metallurgy*, 107(6):373–379.

Roth, H.-C., Prams, A., Lutz, M., Ritscher, J., Raab, M., and Berensmeier, S. (2016). A high-gradient magnetic separator for highly viscous process liquors in industrial biotechnology. *Chemical Engineering and Technology*, 39(3):469–476.

Sellgren, A., Mustafa, A., Addie, G., and Whitlock, L. (2011). Performance of different centrifugal slurry pump impeller configurations when pumping thickened tailings. In *Paste 2011: Proceedings of the 14th International Seminar on Paste and Thickened Tailings*, pages 405–415. Australian Centre for Geomechanics.

Sery, G., Kabamba, B., and Slatter, P. (2006). Paste pumping with centrifugal pumps: evaluation of the hydraulic institute chart de-rating procedures. In *Paste 2006: Proceedings of the Ninth International Seminar on Paste and Thickened Tailings*, pages 403–412. Australian Centre for Geomechanics.

Walker, C. and Goulas, A. (1984). Performance characteristics of centrifugal pumps when handling non-newtonian homogeneous slurries. *Proceedings of the Institution of Mechanical Engineers, Part A: Journal of Power and Energy*, 198(1):41–49.

Wilson, K. C., Addie, G. R., Sellgren, A., and Clift, R. (2006). *Centrifugal Pumps*. Springer.